A novel *CACNA1C* mutation identified in a patient with Timothy syndrome without syndactyly exerts both marked loss- and gain-of-function effects

Junichi Ozawa, MD, PhD,[*†] Seiko Ohno, MD, PhD,[*‡] Hideki Saito, MD,[§] Akihiko Saitoh, MD, PhD,[†] Hiroshi Matsuura, MD, PhD,[‖] Minoru Horie, MD, PhD[*]

*From the *Department of Cardiovascular and Respiratory Medicine, Shiga University of Medical Science, Otsu, Japan, †Department of Pediatrics, Niigata University Graduate School of Medical and Dental Sciences, Niigata, Japan, ‡Center for Epidemiologic Research in Asia, Shiga University of Medical Science, Otsu, Japan, §Department of Cardiology, Seirei Hamamatsu General Hospital, Hamamatsu, Japan, and ‖Department of Physiology, Shiga University of Medical Science, Otsu, Japan.*

Introduction

Timothy syndrome (TS) is a rare multisystem disorder associated with long QT syndrome (LQTS, type 8), congenital heart disease, syndactyly, dysmorphic facial features, and neurologic symptoms including autism, seizures, and intellectual disability.[1] Classical TS is caused by a recurrent *de novo* $Ca_V1.2$ missense mutation, G406R (G1216A transition in the alternatively spliced exon 8a of *CACNA1C*).[1] Despite syndactyly being a common feature of the classical form of TS,[1] 2 atypical patients were found with severe cardiac deficits but without syndactyly.[2] Those patients were identified as carriers of mutations G406R and G402S in the mutually exclusive exon 8, which is more predominantly expressed in the heart. It is thought that the difference in the expression levels between exons 8a and 8 underlies or results in the differential expression of cardiac phenotypes.[1,2]

More recently, 2 classical TS patients were also reported to have other mutations in exons other than exon 8a (A1473G or I1166T),[3,4] though a TS patient without syndactyly carrying the same I1166T was also reported.[5] In addition, patients expressing only LQTS phenotype without extracardiac features have been reported, in whom G402S in exon 8 or other *CACNA1C* mutations were identified (LQT8; LQTS type 8).[4,6–9] *CACNA1C* mutation carriers therefore have various degrees of phenotype expressivity.

In the present study, we analyzed the functional outcome of a novel $Ca_V1.2$ mutation, S643F, identified in a TS proband without syndactyly but with severe cardiac phenotype. We examined the molecular mechanism underlying the mutation.

Case report

The proband, a 14-year-old boy, presented with a prolonged QT interval and dysmorphic facial features—round face, flat nose, and low-set ear—but without syndactyly. Figure 1A is a representative electrocardiogram (ECG) recorded 1 year after the cardiac event that he suffered as described below; QT and QTc intervals were 480 ms and 478 ms, respectively. He was identified to have intellectual disability at age 4 and was diagnosed as autistic spectrum disorder at age 12. He also had a history of seizures. He suffered cardiopulmonary arrest during sleep in the early morning at the age of 13 and was successfully resuscitated by his family. Figure 1B exhibits the ECG recorded a few hours after the resuscitation. The ultrasound echocardiography showed no abnormality including left ventricular dysfunction, congenital heart defects, or hypertrophy. On the third hospital day, ECG showed T-wave inversion in all leads except aV_R (Supplemental Figure 1A), and the echocardiography revealed a left ventricular apical ballooning. As the coronary computerized tomography angiogram showed no occlusion in the coronary artery, he was diagnosed as Takotsubo cardiomyopathy induced by the antecedent cardiac event.[10] Torsades de pointes and subsequent ventricular fibrillation (VF) occurred recurrently on the third hospital day (Supplemental Figure 1B). However, there were no other fatal ventricular arrhythmias after admission, and no antiarrhythmic drugs were introduced. A careful re-evaluation of ECGs recorded at age 6, 9, and 12 all showed QT interval prolongation (QTc = 471–500 ms) and late-onset peaked T. He then underwent an implantable cardioverter-defibrillator placement. During the follow-up

KEYWORDS Electrophysiology; Genetics; Long QT syndrome; L-type calcium channel; Timothy syndrome
(Heart Rhythm Case Reports 2018;4:273–277)

The study was supported in part by MEXT KAKENHI Grant Number 15H04818 (to M.H.) and 15K09689 (to S.O.) from the Ministry of Education, Culture, Sports, Science, and Technology of Japan, and the grant from the Ministry of Health, Labor and Welfare of Japan for Clinical Research on Intractable Disease (H27-032 to M.H.). **Address reprint requests and correspondence:** Dr Minoru Horie, Department of Cardiovascular and Respiratory Medicine, Shiga University of Medical Science, Seta-Tsukinowa, Otsu, Shiga 520-2192, Japan. E-mail address: horie@belle.shiga-med.ac.jp.

https://doi.org/10.1016/j.hrcr.2018.03.003

KEY TEACHING POINTS

- Electrocardiograms in patients with Timothy syndrome patients sometimes present T-wave depolarization pattern similar to long QT syndrome type 3, such as a late-onset peaked T wave.
- We identified a novel *CACNA1C* mutation, S643F, in a 14-year-old boy with Timothy syndrome without syndactyly.
- S643F is located within the $Ca_V1.2$ S4–S5 linker of domain II, and the mutant channel exerts both marked loss-of function and gain-of-function effects.

of 2 years without medication therapy, there was no shock for VF. Family history was negative for sudden cardiac death, LQTS, fatal arrhythmias, or neurological abnormalities.

Genetic test using a panel gene screening identified a novel heterozygous missense *CACNA1C* variant, S643F. This variant was confirmed by the Sanger method (Figure 1C, left). The serine in position 643 is highly conserved among different species (Figure 1C, right). The subsequent genetic test on the patient's parents and siblings revealed that they were all negative for the variant, indicating a *de novo* mutation. Figure 1D illustrates a schematic topology of *CACNA1C* in which all the known TS- and LQT8-related mutations identified so far are highlighted. The variant identified in this study is indicated in red. Serine 643 is located in the intracellular S4–S5 linker of domain II. The variant is located in the inner side of the cell membrane and has not been previously reported in 3 available online databases: Human Genetic Variation Database (http://www.genome.med.kyoto-u.ac.jp/SnpDB/), NHLBI Exome Sequencing Project Exome Variant Server (http://evs.gs.washington.edu/), and 1000 Genomes Browser (http://www.1000genomes.org/).

Using a heterologous expression system, we examined the electrophysiological characteristics of wild-type (WT) and mutant $Ca_V1.2$ channels. Detailed methods on the human embryonic kidney (HEK) cell culture and transfection, as well as subsequent electrophysiological measurements and data analysis, are available in the Supplemental Material. Table 1 summarizes the biophysical parameters measured from multiple cells. Figure 2A depicts nisoldipine (1 μM)-sensitive current traces from 2 different HEK cells expressing *CACNA1C*-WT and S643F mutant channels, respectively (upper), and the lower panel shows that 2 different current traces elicited at 0 mV and +20 mV from a holding potential of −70 mV at baseline showed increased late calcium current of the mutant channel. In Figure 2B, peak inward current

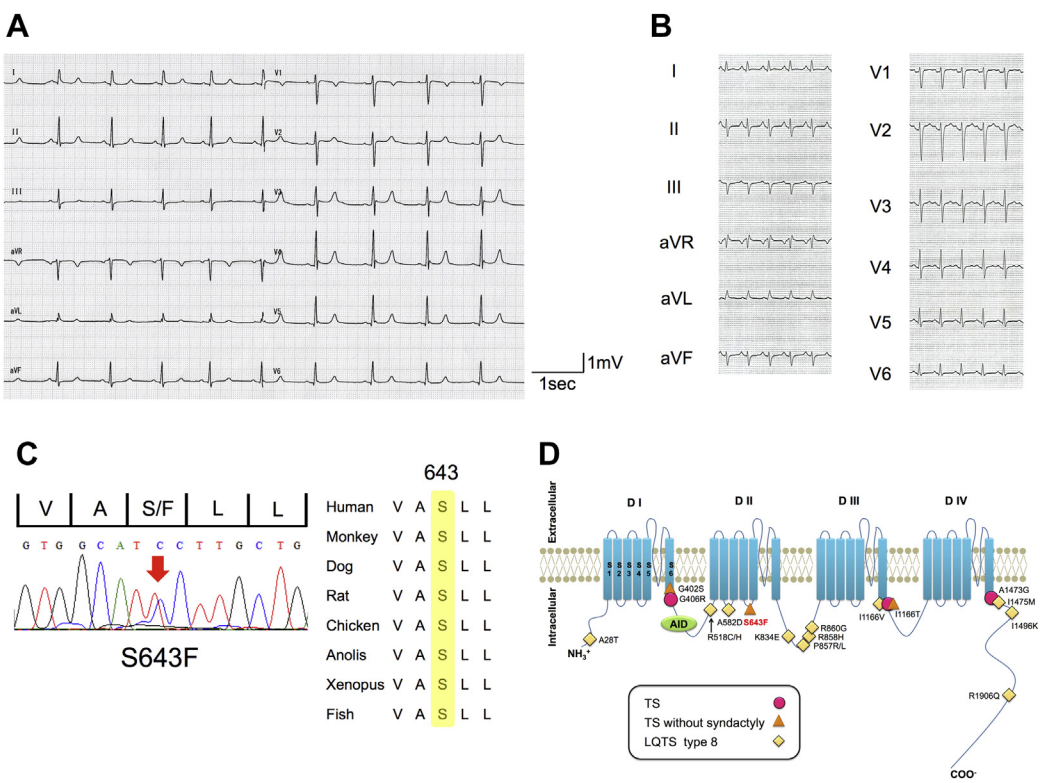

Figure 1 Electrocardiograms. **A:** One year after the cardiac event. **B:** Day of admission. **C:** At left: Electropherograms of p.S643F. At right: Amino acid sequence alignments of p.S643F. **D:** Predicted topology of the $Ca_V1.2$ α subunit. Pink-filled circles indicate positions of mutations causing TS, and orange-filled triangles those of mutations causing TS without syndactyly. Yellow-filled diamonds denote mutations causing only LQTS phenotype without extracardiac features. AID = α1 interacting domain; D = domain; LQTS = long QT syndrome; S = segment; TS = Timothy syndrome.

Table 1 Biophysical parameters of *CACNA1C* WT and mutant channels

Biophysical parameters	WT	S643F
Activation	(n = 18)	(n = 15)
Peak density (pA/pF)	−12.3 ± 0.95	−1.7 ± 0.15*
Vh (mV)	1.9 ± 1.3	−13.5 ± 1.2*
k	7.8 ± 0.23	9.2 ± 0.27*
Conductance	(n = 18)	(n = 15)
*V*rev (mV)	72.5 ± 1.3	70.7 ± 3.2
Peak density (pS)	0.26 ± 0.025	0.048 ± 0.008*
Inactivation	(n = 15)	(n = 11)
Vh (mV)	−11.8 ± 1.4	−13.8 ± 2.0
k	−8.2 ± 1.1	−11.3 ± 2.5*
Time constant (ms)	(n = 18)	(n = 15)
0 mV	49.0 ± 2.1	113.5 ± 4.1*
+10 mV	49.7 ± 1.2	123.0 ± 6.1*
+20 mV	53.9 ± 1.4	130.6 ± 7.9*
+30 mV	61.5 ± 2.3	164.0 ± 13.7*

Peak current density of activation was measured at +20 mV for WT, at 0 mV for S643F, and at +10 mV for R412M. Peak density of conductance was measured at +40 mV.

The number of experiments is indicated in parentheses. Values are represented as means ± SEM.

WT = wild-type.

*$P < .01$ vs WT.

densities are plotted as a function of test potential (I-V relations). While WT (black open circles) reached the peak current at +20 mV, S643F mutants showed a leftward shift of I-V relation, with maximal inward currents at 0 mV. Compared with WT, inward current density in S643F was significantly smaller at potentials between −10 and +40 mV, with 86.2% reduction in peak current density (WT at +20 mV = −12.3 ± 0.95 pA/pF vs S643F at 0 mV = −1.7 ± 0.15 pA/pF, $P < .001$). Figure 2C displays remaining current densities after 500 ms depolarization. Compared with WT, inward current density in S643F was significantly larger at test potentials between +10 and +30 mV.

Figure 2D depicts steady-state activation curves for WT and S643F. Experimental data were fitted with a Boltzmann equation. Activation of S643F mutant channels showed a significant negative shift compared with WT (Table 1). Current decay of expressed calcium current was analyzed by fitting to a single exponential function. In Figure 2E, time constants (τ) thus measured are plotted as a function of test potentials. Compared with WT, they were significantly larger at test potentials between 0 and +30 mV in S643F mutants.

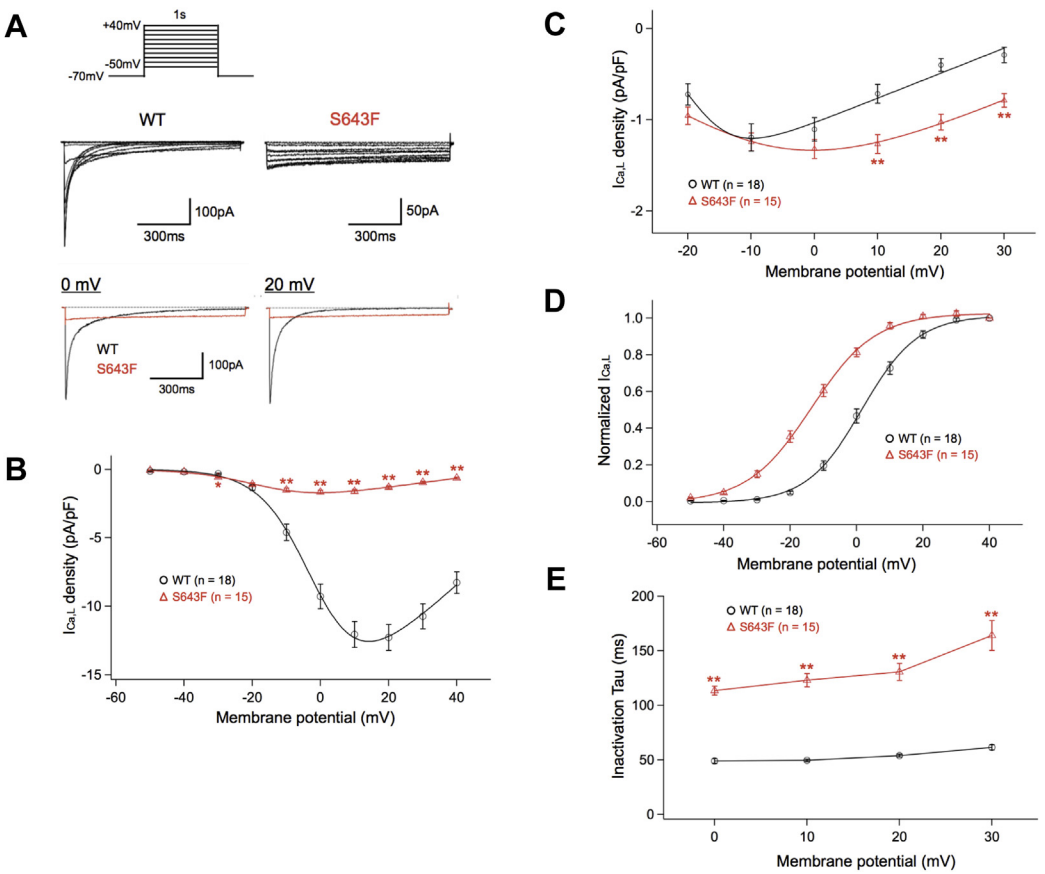

Figure 2 Functional analysis of the mutant $Ca_V1.2$ channels. **A:** Whole-cell current representative recordings of wild-type (WT) and mutant Ca^{2+} channels. Peak inward current-voltage relationships were constructed by applying 1-s pulses from a holding potential of −70 mV to potentials ranging from −50 to +40 mV (upper). Representative traces of currents elicited at 0 mV and +20 mV from a holding potential of −70 mV at baseline (lower). **B:** Peak inward current-voltage relationship for WT (*black circles*, n = 18) and S643F (*red triangles*, n = 15). Peak inward currents were normalized to cell capacitance to give a measure of Ca^{2+} current density. *$P < .05$, **$P < .01$. **C:** The relationship between remaining currents at 500 ms depolarization and voltage for WT (*black circles*, n = 18) and S643F (*red triangles*, n = 15). **D:** Conductance-voltage activation curves for WT (*black circles*, n = 18) and S643F (*red triangles*, n = 15). **E:** Time constants for the voltage dependence of inactivation in WT (*black circles*, n = 18) and S643F (*red triangles*, n = 15). *$P < .05$, **$P < .01$.

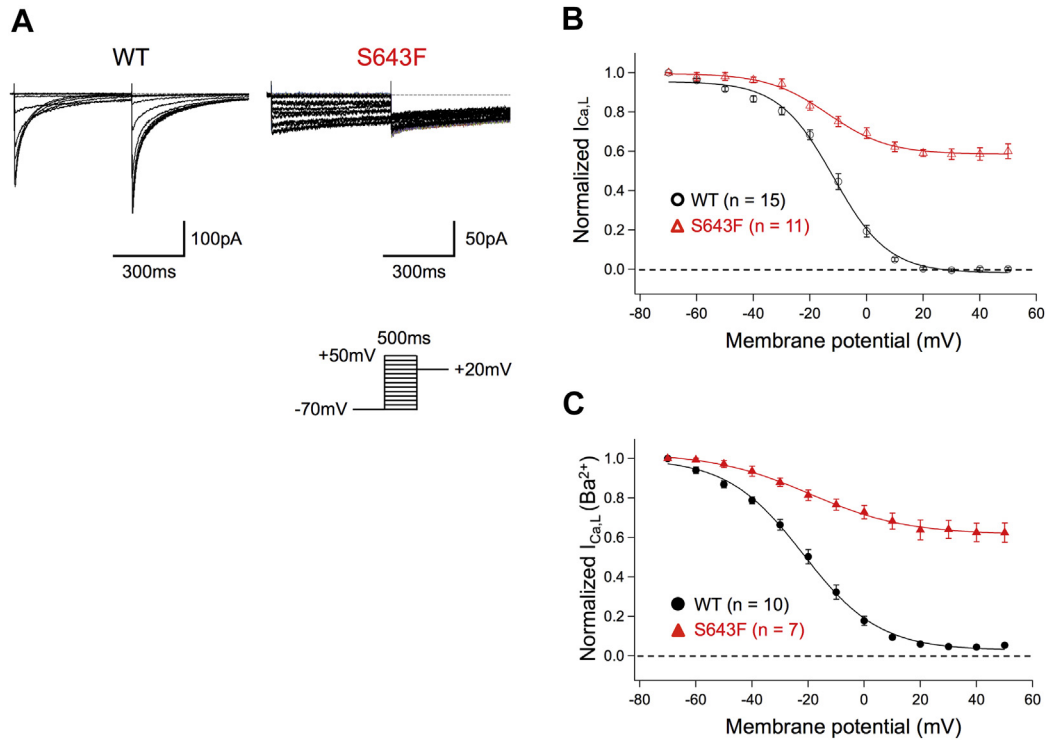

Figure 3 **A:** To study the voltage dependence of inactivation, two-step voltage protocol, as indicated in the bottom right inset, was employed. Upper two sets traces are representative records. **B:** Conductance-voltage inactivation curves of Ca^{2+} current for wild-type (WT) (*black circles*, n = 15) and S643F (*red triangles*, n = 11). **C:** Conductance-voltage inactivation curves of Ba^{2+} current for WT (*black circles*, n = 10) and S643F (*red triangles*, n = 7).

Inactivation gating was evaluated by using a double-pulse method, as shown in the upper panel of Figure 3A. In WT channels, inactivation process was completed at voltages > +20 mV (100%). In contrast, S643F channels never reached a fully inactivated state, and its inactivation level was 42% at maximum (Figure 3B). In order to exclude the Ca-calmodulin-dependent inactivation process and to investigate whether mutant channels primarily defected to voltage-dependent inactivation (VDI) process, we employed Ba as a charge carrier, where Ca-calmodulin-dependent inactivation was largely eliminated. As shown in Figure 3C, WT channels presented a complete inactivation at >+20 mV, while S643F showed significantly impaired inactivation, reaching to the level of inactivation by 38%.

Discussion

In the present study, we demonstrated that a novel *CACNA1C* mutation, S643F, identified in a TS patient exerted an increase in late $Ca_V1.2$ currents. Moreover, the mutant $Ca_V1.2$ channels showed a marked reduction in peak currents, as previously reported in Brugada syndrome, idiopathic VF, or early repolarization syndrome.[11,12]

Mutant S643F $Ca_V1.2$ showed a decreased peak current. S643 is located in the S4–S5 linker of domain II, which may play a part in maintaining normal gating of $Ca_V1.2$. In voltage-gated potassium channels (K_V), the S4–S5 linker plays a crucial role in the electromechanical coupling between S4 and S6: linking the movement of the voltage sensor (S4) to the pore opening via an interaction with the S6 domain, which is pulled open during activation gating.[12] We suspected that a similar gating mechanism might be present in $Ca_V1.2$ channels as well. The substitution of a serine to a phenylalanine might hinder the accurate movement of the activation gate, decreasing the total peak current. Notably, a similar peak current reduction has been observed in other *CACNA1C* mutations detected in Brugada syndrome, idiopathic VF, or early repolarization syndrome patients.[11,12] Therefore, it might be better to avoid taking calcium channel blockers.

In addition, S643F $Ca_V1.2$ showed an extraordinary decrease in VDI. The DI–II linker plays a crucial role for VDI as a hinged-lid gating particle, interacting with the S6 domain.[13,14] There is no report of the interaction between the DI–II linker and the S4–S5 linker, in which S643 is located; therefore the mechanism of a decrease in VDI is still veiled.

Moreover, all TS patients, including our patient, showed a T-wave depolarization pattern similar to LQTS type 3 (LQT3), such as a late-onset peaked T wave (Figure 1).[1–5] This would be a key diagnostic milestone for isolated cardiac phenotype (LQT8).

Conclusion

We identified a novel *CACNA1C* mutation in a TS patient without syndactyly. Our findings expand the spectrum of TS.

Appendix

Supplementary data

Supplementary data associated with this article can be found in the online version at https://doi.org/10.1016/j.hrcr.2018.03.003.

References

1. Splawski I, Timothy KW, Sharpe LM, et al. $Ca_v1.2$ calcium channel dysfunction causes a multisystem disorder including arrhythmia and autism. Cell 2004; 119:19–31.
2. Splawski I, Timothy KW, Decher N, Kumar P, Sachse FB, Beggs AH, Sanguinetti MC, Keating MT. Severe arrhythmia disorder caused by cardiac L-type calcium channel mutations. Proc Natl Acad Sci U S A 2005;102:8089–8096.
3. Gillis J, Burashnikov E, Antzelevitch C, Blaser S, Gross G, Turner L, Babul-Hirji R, Chitayat D. Long QT, syndactyly, joint contractures, stroke and novel CACNA1C mutation: expanding the spectrum of Timothy syndrome. Am J Med Genet 2012;158A(1):182–187.
4. Boczek NJ, Miller EM, Ye D, Nesterenko VV, Tester DJ, Antzelevitch C, Czosek RJ, Ackerman MJ, Ware SM. Novel Timothy syndrome mutation leading to increase in CACNA1C window current. Heart Rhythm 2015;12:211–219.
5. Wemhoner K, Friedrich C, Stallmeyer B, Coffy AJ, Grace A, Zumhagen S, Seebohm G, Ortiz-Bonnin B, Rinne S, Sachse FB, Schulze-Bahr E, Decher N. Gain-of-function mutations in the calcium channel CACNA1C (Cav1.2) cause non-syndromic long-QT but not Timothy syndrome. J Mol Cell Cardiol 2015; 80:186–195.
6. Boczek NJ, Best JM, Tester DJ, Giudicessi JR, Middha S, Evans JM, Kamp TJ, Ackerman MJ. Exome sequencing and systems biology converge to identify novel mutations in the L-type calcium channel, CACNA1C, linked to autosomal dominant long QT syndrome. Circ Cadiovasc Genet 2013; 6:279–289.
7. Fukuyama M, Wang Q, Kato K, Ohno S, Ding WG, Toyoda F, Itoh H, Kimura H, Makiyama T, Ito M, Matsuura H, Horie M. Long QT syndrome type 8: novel CACNA1C mutations causing QT prolongation and variant phenotypes. Europace 2014;16:1828–1837.
8. Boczek NJ, Ye D, Jin F, Tester DJ, Huseby A, Bos JM, Johnson AJ, Kanter R, Ackerman MJ. Identification and functional characterization of a novel CACNA1C-mediated cardiac disorder characterized by prolonged QT intervals with hypertrophic cardiomyopathy, congenital heart defects, and sudden cardiac death. Circ Arrhythm Electrophysiol 2015;8:1122–1132.
9. Hiippala A, Tallila J, Myllykangas S, Koskenvuo JW, Alastalo TP. Expanding the phenotype of Timothy syndrome type 2: an adolescent with ventricular fibrillation but normal development. Am J Med Genet Part A 2015;167A:629–634.
10. Dawson DK. Acute stress-induced (takotsubo) cardiomyopathy. Heart 2018; 104(2):96–102.
11. Antzelevitch C, Pollevick GD, Cordeiro JM, et al. Loss-of-function mutations in the cardiac calcium channels underlie a new clinical entity characterized by ST-segment elevation, short QT intervals, and sudden cardiac death. Circulation 2007;115:442–449.
12. Burashnikov E, Pfeiffer R, Barajas-Martinez H, et al. Mutations in the cardiac L-type calcium channel associated with inherited J-wave syndromes and sudden cardiac death. Heart Rhythm 2010;7:1872–1882.
13. Stotz SC, Jarvis SE, Zamponi GW. Functional roles of cytoplasmic loops and pore lining transmembrane helices in the voltage-dependent inactivation of HVA calcium channels. J Physiol 2004;554:263–273.
14. Stotz SC, Hamid J, Spaetgens RL, Jarvis SE, Zamponi GW. Fast inactivation of voltage-dependent calcium channels. J Biol Chem 2000; 275:24575–24582.